ChemComm

COMMUNICATION

View Article Online
View Journal

Cite this: DOI: 10.1039/d6cc02481e

Received 22nd April 2026,
Accepted 4th June 2026

DOI: 10.1039/d6cc02481e

rsc.li/chemcomm

Vibrational solvatochromism of rhodium pybox carbonyl complexes mediated by hydrogen bonding

Nil Roig, [ab] Mercedes Alonso *[b] and Adrian B. Chaplin *[a]

The carbonyl stretching frequencies of structurally related classical and non-classical rhodium carbonyl complexes are significantly red-shifted by methanol enrichment in solution and rationalised in terms of the nature of the hydrogen bonding interactions involved using *ab initio* molecular dynamics simulations.

The ν(CO) vibrational frequencies of metal-carbonyl complexes are key spectroscopic handles in organometallic chemistry, facilitating reaction monitoring and providing insight into the metal-mediated activation of CO.[1] Terminal CO coordination is classically characterised by red-shifted values of ν(CO) relative to free CO and interpreted using the Dewar–Chatt–Duncanson bonding model, wherein the CO bond is weakened by population of the π*(CO) orbitals through metal-to-ligand π-backbonding.[2] Contemporary theoretical analysis indicates that this charge transfer occurs alongside significant polarisation of the CO bond,[3] which renders ν(CO) sensitive to the local electrostatic environment and helps reconcile the existence of non-classical carbonyl complexes that exhibit shorter CO bond lengths and blue-shifted ν(CO) values relative to free CO (2143 cm^{-1}).[4,5] As the majority of organometallic chemistry is conducted in solution and the associated intermolecular interactions are primarily electrostatic in nature,[6] it is imperative that solvent effects are considered when interpreting differences in ν(CO).[7] Building upon our recent work investigating the role of electrostatics in metal-carbonyl bonding,[5,8] we herein present a combined experimental and computational study examining how solvent influences the ν(CO) vibrational frequencies of the homologous rhodium(I) and rhodium(III) pybox carbonyl complexes **1** and **2** (Fig. 1). These complexes are an interesting test set as, when analysed by FT-IR spectroscopy in the routinely employed solvent dicholoromethane, the latter is characterised as a non-classical carbonyl complex with ν(CO) = 2151 cm^{-1}.[9]

Inspired by experimental and computational work on conceptually related organocarbonyl compounds, where values of ν(CO) are lowered in hydrogen bonding environments,[10] we have analysed **1** and **2** by FT-IR spectroscopy in binary mixtures of dichloromethane/methanol (Fig. 1). Red shifts are observed as concentration of the strongly H-bonding solvent methanol was increased, with ν(CO) ranging from 2018.6 to 2008.5 cm^{-1} for **1** ($\Delta\nu$(CO) = −10.1 cm^{-1}) and 2151.2 to 2135.5 cm^{-1} for **2** ($\Delta\nu$(CO) = −15.7 cm^{-1}). Similar differences are observed for

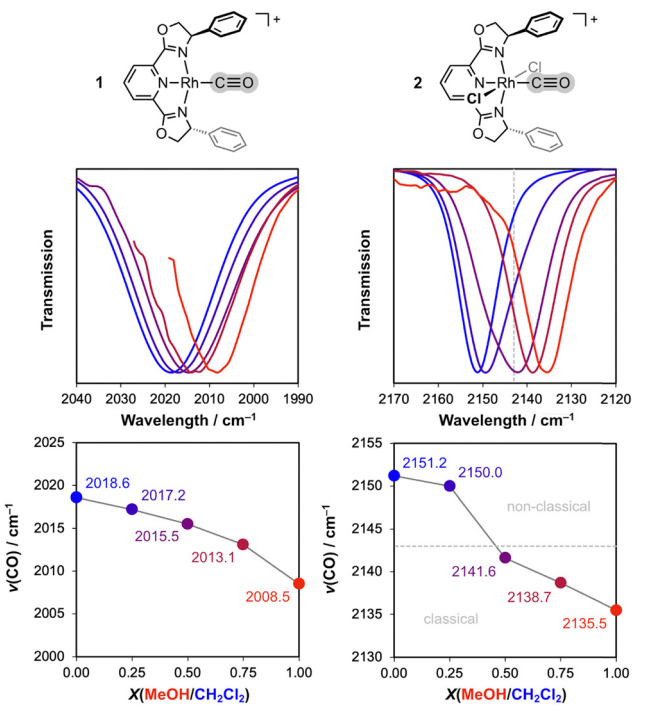

Fig. 1 FT-IR analysis of rhodium(I) and rhodium(III) pybox carbonyl complexes **1** and **2** in binary mixtures of dichloromethane/methanol. $[BAr_4^F]^-$ counterions omitted for clarity.

[a] *Department of Chemistry, University of Warwick, Coventry CV4 7AL, UK. E-mail: a.b.chaplin@warwick.ac.uk*

[b] *Eenheid Algemene Chemie (ALGC), Vrije Universiteit Brussel (VUB), 1050 Brussels, Belgium. E-mail: mercedes.alonso.giner@vub.be*

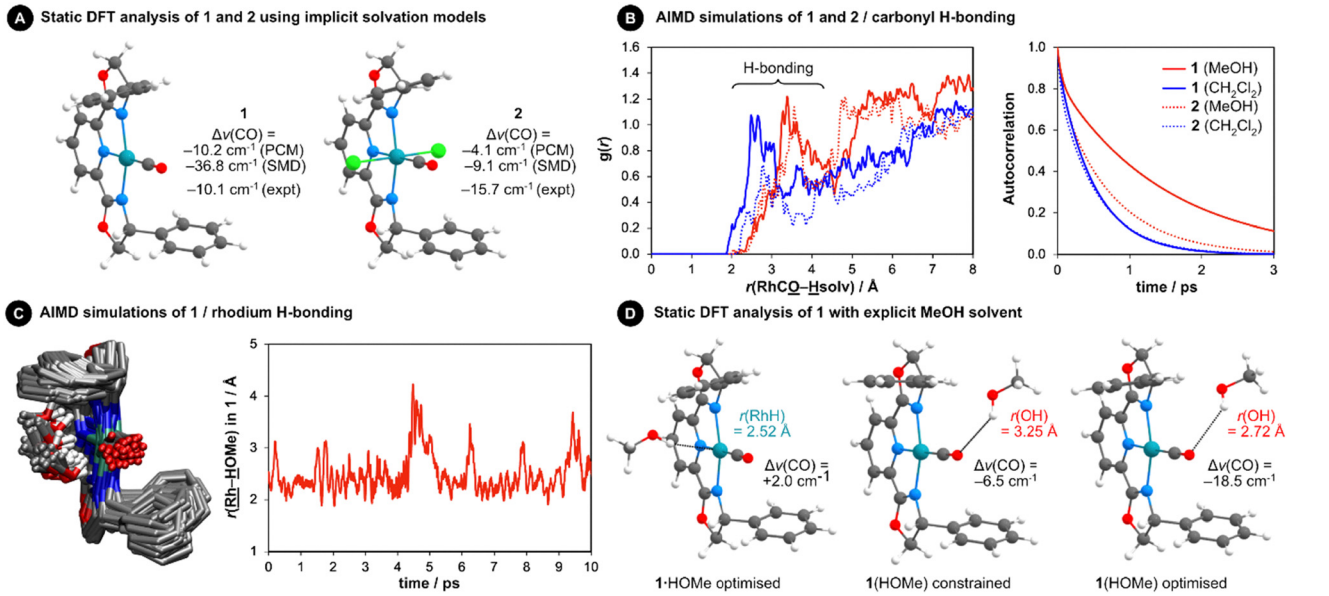

Fig. 2 Computational analysis of rhodium(I) and rhodium(III) pybox carbonyl complexes **1** and **2** relevant to their observed vibrational solvatochromism in methanol *vs.* dichloromethane (cations only). Static DFT calculations were performed at the B3PW91/6-31G(d,p) (SDD for Rh) level of theory.[13,14] AIMD simulations were performed using the PBE functional and the DZVP-MOLOPT-GTH (DZVP-MOLOPT-SR-GTH for Rh) Gaussian plane-wave basis set, with the cut-off and relative cut-off set at 250 Ry and 80 Ry respectively, and dispersion effects captured through inclusion of Grimme's D3 dispersion correction.[15] $\Delta\nu$(CO) for MeOH *vs.* CH_2Cl_2 (A) and explicit MeOH *vs.* gas phase (D).

the dimethyl-pybox analogues of **1** ($\Delta\nu$(CO) = −12.3 cm^{-1}) and **2** ($\Delta\nu$(CO) = −13.9 cm^{-1}). The concave shape of the solvatochromic curve indicates that **1** is preferentially solvated by dichloromethane, while the point of inflection observed for **2** is attributed to dielectric enrichment and a reduced propensity for H-bonding.[11] The observed $\Delta\nu$(CO) are substantial and can be put in context by reference to the 11 cm^{-1} difference in Tolman Electronic Parameter between the aryl and alkyl phosphines PPh_3 and PCy_3.[12] Remarkably for **2** the red shift is large enough to merit a change in classification from a non-classical carbonyl complex in dichloromethane to a classical carbonyl complex in methanol.

Static DFT calculations using implicit solvation models failed to consistently reproduce the red shifts observed in pure methanol relative to dichloromethane (Fig. 2A).[13] Specifically, $\Delta\nu$(CO) for **2** is underestimated by the polarizable continuum model (PCM), whereas that of **1** is overestimated by the solvation model based on density (SMD).[14] Both implicit models predict the rhodium(I) complex **1** to be more solvatochromic than the rhodium(III) complex **2**, contrary to experiment but consistent with how ν(CO) of these complexes are affected by an oriented external electric field (see SI, Fig. S18).

To more accurately capture solvation effects, we resorted to DFT-based *ab initio* molecular dynamics (AIMD) simulations, where dichloromethane or methanol molecules surrounding **1** and **2** are explicitly included in the calculations. The level of theory was selected based on previous work,[5,15] with simulations performed in the NVT ensemble at 298 K with a 0.5 fs time step, consistent with the timescale of an IR experiment. An equilibration phase of 5000 steps preceded a production run of 20 000 steps. Wannier-based analysis on the final 10 000 steps enabled ensemble calculation of ν(CO), with the resulting $\Delta\nu$(CO) values in excellent agreement with experiment (−9.8 *cf.* −10.1 cm^{-1} for **1**; −16.3 *cf.* −15.7 cm^{-1} for **2**).[16] Radial distribution functions traced between the carbonyl O atom and solvent protons revealed H-bonding interactions for **1** and **2**, with peaks between 2–3 Å for dichloromethane and 3–4 Å for methanol (Fig. 2B). The lifetime of these interactions, as quantified by an autocorrelation analysis,[16] show that methanol forms stronger, longer-lived H-bonds than dichloromethane, congruent with the red-shifted values of ν(CO) measured experimentally in methanol (τ = 2.5 *vs.* 0.9 ps for **1**; τ = 1.2 *vs.* 0.9 ps for **2**; Fig. 2B). All else being equal, the larger increase in H-bonding lifetime calculated for **1** ($\tau_{MeOH}/\tau_{CH_2Cl_2}$ = 2.7) than for **2** ($\tau_{MeOH}/\tau_{CH_2Cl_2}$ = 1.3) is, however, at odds with the magnitudes of $\Delta\nu$(CO) measured experimentally, which imply the opposite trend.

From closer inspection of the AIMD trajectories, a persistent H-bond with the metal centre was uniquely identified for **1** in methanol (Fig. 2C). This solvent interaction is maintained throughout the entire simulation run, albeit for one reversible decoordination of <1 ps, and characterised by an average Rh···H–O distance of 2.5(4) Å. To assess the impact on the value of ν(CO), the geometry of this methanol adduct **1**·HOMe was extracted from the trajectory and analysed in the gas-phase using static DFT methods (Fig. 2D). The H-bond was retained upon optimisation and is characterised by a Rh···H contact of 2.52 Å and a Rh···H–O angle of 141°. Subsequent Hessian analysis indicates that formation of **1**·HOMe induces a blue-shift in ν(CO) of +2.0 cm^{-1} relative to **1**.[17] Following a similar static DFT analysis, red shifts in ν(CO) but of greater magnitude are calculated for carbonyl H-bonding using an explicit molecule of methanol, either constrained based on the AIMD data or

in a fully optimised geometry (Fig. 2D and Fig. S20). It therefore appears that the solvatochromic response for **1** in methanol reflects a balance between relatively short-lived H-bonding of the solvent with the carbonyl ligand, which induce large red-shifts in ν(CO) and more persistent H-bonding with the metal centre, which counteract lowering in ν(CO).

This experimental/computational investigation reinforces the importance of electrostatics in metal-carbonyl bonding and, through examining changes in the ν(CO) vibrational frequency, demonstrates how activation of CO can be modulated by interaction with the solvent. The latter is exemplified by rhodium(III) complex **2**, for which vibrational solvatochromism in dichloromethane/methanol spans the non-classical/classical divide, and underscores why accurate comparison of ν(CO) values requires measurements to be made in the same solvent.[7] More broadly, our results show that solvent-induced spectral changes of metal carbonyl complexes can be understood in terms of dynamic H-bonding interactions and their lifetimes, as revealed by *ab initio* molecular dynamics simulations in combination with snapshot analysis by traditional, static DFT calculations.

Conflicts of interest

There are no conflicts to declare.

Data availability

The data supporting this article have been included as part of the supplementary information (SI): synthesis and characterisation of the dimethyl pybox analogues of **1** and **2**, computational information and data, optimised geometries in XYZ format. See DOI: https://doi.org/10.1039/d6cc02481e.

CCDC under 2545198 (**1**) and 2545199 (**2**) contain the supplementary crystallographic data for this paper.[18]

Acknowledgements

We thank the EUTOPIA alliance (N. R.), Vrije Universiteit Brussel (M. A.) and University of Warwick (A. B. C.) for financial support. Computational resources and services were provided by the Shared ICT Services Centre funded by the VUB, the Flemish Supercomputer Center (VSC), and FWO.

References

1 J. F. Hartwig, *Organotransition Metal Chemistry – From Bonding to Catalysis*, University Science Books, 2010; *Comprehensive Organometallic Chemistry IV*, ed. G. Parkin, K. Meyer, D. O'Hare, Elsevier, 2022.
2 M. J. S. Dewar, *Bull. Soc. Chim. Fr.*, 1951, **18**, C79; J. Chatt and L. A. Duncanson, *J. Chem. Soc.*, 1953, 2939–2947; D. M. P. Mingos, *J. Organomet. Chem.*, 2001, **635**, 1–8.
3 A. S. Goldman and K. Krogh-Jespersen, *J. Am. Chem. Soc.*, 1996, **118**, 12159–12166; A. J. Lupinetti, S. Fau, G. Frenking and S. H. Strauss, *J. Phys. Chem. A*, 1997, **101**, 9551–9559; E. Rossomme, C. N. Lininger, A. T. Bell, T. Head-Gordon and M. Head-Gordon, *Phys. Chem. Chem. Phys.*, 2020, **22**, 781–798; S. C. C. van der Lubbe, P. Vermeeren, C. F. Guerra and F. M. Bickelhaupt, *Chem. – Eur. J.*, 2020, **26**, 15690–15699; J. Han, A. Grofe and J. Gao, *Inorg. Chem.*, 2021, **60**, 14060–14071; G. Bistoni, S. Rampino, N. Scafuri, G. Ciancaleoni, D. Zuccaccia, L. Belpassi and F. Tarantelli, *Chem. Sci.*, 2016, **7**, 1174–1184.
4 G. N. Phillips, M. L. Teodoro, T. Li, B. Smith and J. S. Olson, *J. Phys. Chem. B*, 1999, **103**, 8817–8829; E. S. Park, S. S. Andrews, R. B. Hu and S. G. Boxer, *J. Phys. Chem. B*, 1999, **103**, 9813–9817; E. S. Park and S. G. Boxer, *J. Phys. Chem. B*, 2002, **106**, 5800–5806.
5 G. L. Parker, R. V. Lommel, N. Roig, M. Alonso and A. B. Chaplin, *Chem. – Eur. J.*, 2022, **28**, e202202283.
6 S. D. Fried and S. G. Boxer, *Acc. Chem. Res.*, 2015, **48**, 998–1006.
7 C. C. Barraclough, J. Lewis and R. S. Nyholm, *J. Chem. Soc.*, 1961, 2582–2584; G. Bor, *Spectrochim. Acta*, 1962, **18**, 817–822; R. J. H. Clark and B. Crociani, *Inorg. Chim. Acta*, 1967, **1**, 12–16; C. S. Creaser, M. A. Fey and G. R. Stephenson, *Spectrochim. Acta, Part A*, 1994, **50**, 1295–1299; C. J. Huber, T. C. Anglin, B. H. Jones, N. Muthu, C. J. Cramer and A. M. Massari, *J. Phys. Chem.*, 2012, **116**, 9279–9286; B. H. Jones, C. J. Huber and A. M. Massari, *J. Phys. Chem. A*, 2013, **117**, 6150–6157.
8 N. Roig, R. V. Lommel, M. Alonso and A. B. Chaplin, *Organometallics*, 2024, **43**, 2787–2796.
9 G. L. Parker, S. Lau, B. Leforestier and A. B. Chaplin, *Eur. J. Inorg. Chem.*, 2019, 3791–3798.
10 C. Reichardt and T. Welton, *Solvents and Solvent Effects in Organic Chemistry*, Wiley-VCH, 4th edn, 2003, pp 397–403; S. D. Fried, S. Bagchi and S. G. Boxer, *J. Am. Chem. Soc.*, 2013, **135**, 11181–11192.
11 C. Lerf and P. Suppan, *J. Chem. Soc., Faraday Trans.*, 1992, **88**, 963–969.
12 C. A. Tolman, *Chem. Rev.*, 1977, **77**, 313–348.
13 R. Ditchfield, W. J. Hehre and J. A. Pople, *J. Chem. Phys.*, 1971, **54**, 724–728; A. D. Becke, *Phys. Rev. A*, 1988, **38**, 3098–3100; D. Andrae, U. Häußermann, M. Dolg, H. Stoll and H. Preuß, *Theor. Chim. Acta*, 1990, **77**, 123–141; A. W. Ehlers, M. Böhme, S. Dapprich, A. Gobbi, A. Höllwarth, V. Jonas, K. F. Köhler, R. Stegmann, A. Veldkamp and G. Frenking, *Chem. Phys. Lett.*, 1993, **208**, 111–114; A. D. Becke, *J. Chem. Phys.*, 1993, **98**, 5648–5652.
14 S. Miertuš, E. Scrocco and J. Tomasi, *Chem. Phys.*, 1981, **55**, 117–129; J. Tomasi, B. Mennucci and R. Cammi, *Chem. Rev.*, 2005, **105**, 2999–3094; A. V. Marenich, C. J. Cramer and D. G. Truhlar, *J. Phys. Chem. B*, 2009, **113**, 6378–6396.
15 J. P. Perdew, K. Burke and M. Ernzerhof, *Phys. Rev. Lett.*, 1996, **77**, 3865–3868; J. VandeVondele and J. Hutter, *J. Chem. Phys.*, 2007, **127**, 114105; S. Grimme, J. Antony, S. Ehrlich and H. Krieg, *J. Chem. Phys.*, 2010, **132**, 154104.
16 M. Brehm, M. Thomas, S. Gehrke and B. Kirchner, *J. Chem. Phys.*, 2020, **152**, 164105.
17 Blue shifts of similar magnitude are calculated at the B3PW91/6-31++G(d,p) (SDD for Rh), B3PW91-D3BJ/6-31G(d,p) (SDD for Rh) and ωB97X-D/6-31G(d,p) (SDD for Rh) levels of theory. Further details provided in SI.
18 CCDC 2545198: Experimental Crystal Structure Determination, 2026, DOI: 10.5517/ccdc.csd.cc2rfh5w; CCDC 2545199: Experimental Crystal Structure Determination, 2026, DOI: 10.5517/ccdc.csd.cc2rfh6x.